Thermochimica Acta 481 (2009) 12–19

Contents lists available at ScienceDirect

Thermochimica Acta

journal homepage: www.elsevier.com/locate/tca

Thermal magnetic investigation of the decomposition of $Ni_xMn_{1-x}C_2O_4{\cdot}2H_2O$

B. Donkova[a,*], B. Kotzeva[b], P. Vasileva[a], D. Mehandjiev[b]

[a] Department of Inorganic Chemistry, Faculty of Chemistry, University of Sofia, 1 J. Bourchier Av., Sofia 1164, Bulgaria
[b] Institute of General and Inorganic Chemistry, Bulgarian Academy of Science, Acad. G. Bonchev Str., bl 11, Sofia 1113, Bulgaria

ARTICLE INFO

Article history:
Received 3 August 2008
Received in revised form
14 September 2008
Accepted 17 September 2008
Available online 2 October 2008

Keywords:
Decomposition
Magnetic properties
Solid solutions
Thermal analysis

ABSTRACT

The systems $Ni_xMn_{1-x}C_2O_4{\cdot}2H_2O$ ($x = 0.11$, 0.34) are characterized by XRD, SEM, TG/DTA, EGA-MS and magnetic measurements. The last confirmed that the studied samples are real solid solutions. The SEM reveals that the morphology depends on both the excess of $C_2O_4^{2-}$ and the initial ratio Ni/Mn. The thermal magnetic investigations (*in situ*) show that: (i) the presence of Ni in $Ni_xMn_{1-x}C_2O_4{\cdot}2H_2O$ leads to decreasing in the decomposition temperature in regard to that of the manganese oxalate; (ii) upon increasing the Ni content the temperature of decomposition (in air) is growing up; (iii) the presence of Ni stabilizes the manganese with respect to oxidation, in spite of the occurring process of decomposition.

1. Introduction

During the last years the interest in the utilization of 3d-transition metal oxalates of the so-called "magnesium series" (Mg, Mn, Fe, Co, Ni, Zn) as precursors for oxide materials has been growing considerably. The reasons for this are the following: (i) the low temperature of decomposition; (ii) the liberation of a large amount of volatile substances—H_2O, CO_2 and CO, resulting in final products of highly developed specific surface area; (iii) their isostructural feature leading to their co-crystallization. The latter fact enables obtaining various ratios between the metal ions in the oxalate precursor with high precision, as well as achieving their uniform distribution in the crystal lattice. This option is especially important in view of obtaining spinels. There is a great interest in the system Ni(II)–Mn(II)–C_2O_4–H_2O and in the stoichiometric and non-stoichiometric spinels obtained from it [1–18]. They exhibit a negative temperature coefficient of resistance [12–16] as well as a catalytic activity [17,18].

In order to use the oxalates as precursors it is necessary to control the initial composition, to know well their crystallographic structure, the influence of the conditions of preparation and the mechanism of decomposition. The changes in the parameters of the crystal lattice and the thermal behavior of the precursor $Ni_xMn_{1-x}C_2O_4{\cdot}2H_2O$ were observed as a function of the ratio nickel–manganese as early as in one of the first works [3]. The studies [6,7] considered the effect of different amounts of Cu or Zn on the crystallographic structure of the oxalate phase [7], as well as on the morphology and thermal behavior [6,7]. The work [4] monitored the influence of the hydrodynamic conditions of the synthesis upon the shape and size of $Ni_xMn_{(1-x)}C_2O_4{\cdot}2H_2O$ ($x = 0.24$) by carrying out the synthesis in different types of reactors. It has been pointed out that the difference in the homogeneity of the precursor in shape and size is connected with the stages of formation of the solid phase (nucleus formation, growth, agglomeration). As the conditions of obtaining the precursor exert substantial influence on the technological properties of the oxide materials it is of essential importance to know the factors, which are controlling them. This has not been commented so far in the literature what is the influence of the surplus of oxalate ions on the structure, morphology and thermal behavior of $Ni_xMn_{1-x}C_2O_4{\cdot}2H_2O$ However in Ref. [19] it has been shown that the concentration of the oxalate ions and the time of contact with the mother solution is the basic factor determining the polymorphous form of the oxalates of the magnesium series. Our investigations on the mechanism of inclusion of 3d-elements (Mn, Ni, Co, Cu) in the zinc oxalate dihydrate [20] have established that the co-crystallization processes are also connected with the concentration of $C_2O_4^{2-}$ ions in the initial system.

As it was stated above, in case of using 3d-transition metal oxalates as precursors it is very important to know the process of decomposition. A series of investigations have been reported on this topic—most of them summarized in Refs. [21,22]. A specific feature of these systems is the liberated CO, which is capable of reducing the obtained oxide. This way the oxide with a lower oxidation state

* Corresponding author. Tel.: +359 2 8161214; fax: +359 2 8705024.
E-mail addresses: nhbd@inorg.chem.uni-sofia.bg, nhbd@wmail.chem.uni-sofia.bg (B. Donkova).

0040-6031/$ – see front matter © 2008 Elsevier B.V. All rights reserved.
doi:10.1016/j.tca.2008.09.021

of M^{n+} could be formed and even a metal phase could appear (Ni, Co, Cu oxalates). This is an important point, as the obtained product will include in its composition 3d-metal ions in different oxidation states and coordination, as it is shown in [23–25].

As far as the system $Ni_xMn_{1-x}C_2O_4{\cdot}2H_2O$ is concerned the processes of isothermal and non-isothermal decomposition have been reported in a number of works [1,3–9], and the obtained oxide products have been studied and characterized in [1–11]. It has been established that in the case of decomposition of a mechanical mixture of nickel oxalate and manganese oxalate a new mixture is obtained containing Mn_xO_y ($x \leq y$) and metallic Ni or NiO depending on the atmosphere and on the temperature. On the other hand, in the case of $Ni_xMn_{1-x}C_2O_4{\cdot}2H_2O$ the transformation passes through non-stoichiometric spinel, ilmenite and again a spinel, in which the couples Ni^{2+}/Ni^{3+} are presented, as well as couples Mn^{n+}/Mn^{m+} (n, $m = 2–4$; $n \neq m$). For this reason these products display a good electroconductivity and catalytic activity. When $Ni_xMn_{1-x}C_2O_4{\cdot}2H_2O$ is decomposed in argon atmosphere the reaction products are MnO and Ni [1,3].

The aim of the present work was to supplement the data from previous investigations on the nickel–manganese oxalate by tracing the mechanism of its decomposition using monitoring the magnetic properties *in situ*. On the basis of the changes in the magnetic susceptibility, calculation of the magnetic moment and the constant of Weiss one can observe the change in the oxidation state, in the coordination and interaction of ions in the precursor in the course of the decomposition process [23–25]. Such an investigation, combined with TGA, DTA and mass-spectral analysis of the liberated gases (EGA), enables establishing the decomposition mechanism. In order to obtain information on the influence of the oxalate ions surplus on the type of the obtained precursor and on its properties the synthesis is carried out in excess of $C_2O_4^{2-}$. This way it could be checked if the correlations between the thermal behavior and ratio nickel–manganese, established in [3], are also preserved.

The nickel–manganese oxalate was chosen as the object of this study in view of the option to apply the prepared oxides in the field of catalysis and electronics.

2. Experimental

A series of samples was obtained and two of the samples having a composition $Ni_{0.34}Mn_{0.66}C_2O_4{\cdot}2H_2O$ (phase I) and $Ni_{0.11}Mn_{0.89}C_2O_4{\cdot}2H_2O$ (phase II) were chosen. For the sake of comparison a mechanical mixture was also prepared with a composition $NiC_2O_4{\cdot}2H_2O$:$MnC_2O_4{\cdot}2H_2O$ = 1:1, consisting of individually synthesized oxalates. The synthesis of all the samples has been carried out under the same conditions: two-stream precipitation at temperature 25.0 ± 0.5 °C, electromechanical stirring, pH value after mixing 3.00 ± 0.05. The latter value was achieved by adding the necessary quantity diluted H_2SO_4 or KOH to the initial solutions of $MnSO_4$ and $K_2C_2O_4$. In the synthesis of mixed phases 1 h after the beginning the precipitated solid phases are filtered off. The obtained samples are subjected to X-ray analysis, microscope observation, thermal analyses, EGA-MS and magnetic measurements.

The microscope observation has been carried out by means of an optical microscope Carl Zeiss—Jena and scanning electron microscope JSM-5510.

The XRD analysis was carried out with a D 500 Siemens powder diffractometer using Cu Kα radiation in a 2θ diffraction interval of 10–60°. The identification of the phases was realized by means of the database JCPDS—International Center for Diffraction Data. The diffraction data were processed using the Powder Cell program [26].

The thermal investigations were performed on a Paulik-Erdey MOM OD-102 derivatograph. The DTA and TG curves were obtained in a static air atmosphere with sample mass of 0.200 g at a heating rate of 10 °C/min in the 25–1000 °C temperature range, using a standard corundum crucible. The reference sample was pure α-Al_2O_3.

The mass-spectral analysis of the gases evolved from samples by thermal decomposition in vacuum was performed with the aid of a magnetic mass-spectrometer MS10 AEI. Standard parameters (a filament current of 50 μA and an ionizing voltage of 70 V) were applied to the ion source of the mass-spectrometer. The energy of the electrons in the ion source is 70 eV. The mass-spectral investigations were carried out applying linear temperature program. Thus the kinetic curve of the process was obtained. For this purpose the sample (≤1 mg) was placed in a quartz reactor, the analytical system for gas analysis was evacuated ($p \leq 1 \times 10^{-3}$ Torr) and then the heating was switched on. The temperature was being increased gradually from room temperature (20 °C) up to about 700 °C at a rate of 10°/min. Throughout this time interval the mass-spectral peaks $m/z = 28$ (of CO) and $m/z = 44$ (of CO_2) were being registered. The water, liberated during dehydration of the oxalates, was accumulated in a trap, kept at a temperature of −117 °C (melting ether bath). After switching off the heating the quantity of the liberated gases was determined by means of an internal standard (^{40}Ar), while the frozen water was being vaporized and it was measured manometrically (silicon-oil manometer). The background mass-spectrum was recorded before starting the heating.

The magnetic measurements are carried out in accordance with the method, described in [23,24]. The specific magnetic susceptibility of the sample was studied in the temperature range 25–300 °C with a Faraday type of magnetic balance by a stepwise increase of the temperature. At each step, the temperature was kept constant for 30 min before starting the measurements. The respective weight losses were also determined.

The effective magnetic moments of the samples were calculated on the basis of the Curie–Weiss law, using the values of the magnetic susceptibilities.

In case of *in situ* measurements, the magnetic moments were calculated as:

$$\mu_{\text{eff}} = 2.828 = [\chi(T - \theta)]^{1/2} \quad (1)$$

where μ_{eff} is the effective magnetic moment in Bohr's magneton, BM; χ is the molar magnetic susceptibility; T is the absolute temperature in K; θ is the Weiss constant in K.

3. Experimental results and discussion

3.1. X-ray diffraction analysis

Fig. 1 shows the X-ray diffraction patterns of the synthesized $NiC_2O_4{\cdot}2H_2O$ (a) and $MnC_2O_4{\cdot}2H_2O$ (b), their mechanical mixture (c) and the obtained $Ni_xMn_{1-x}C_2O_4{\cdot}2H_2O$ samples (d and e). Peaks of the two ingredient phases are clearly discernible in the mechanical mixture, while the diffraction patterns of the mixed systems show that the latter represent real solid solutions. About the polymorphous form (monoclinic α or orthorhombic β), in which the solid solutions $Ni_xMn_{1-x}C_2O_4{\cdot}2H_2O$ are crystallizing, the data available in the literature are as follows: according to Töpfer [3] they crystallize in the monoclinic α-form within the interval $0.17 \leq x \leq 0.86$, studied by him. In the study [4] it is stated that a phase with composition $Ni_{0.24}Mn_{0.76}C_2O_4{\cdot}2H_2O$ is iso-structural with respect to the monoclinic α-$MnC_2O_4{\cdot}2H_2O$. In Ref. [6] the THESIS of Metz is cited, in which it is established that solid solutions with nickel content $x \leq 0.25$ crystallize in the

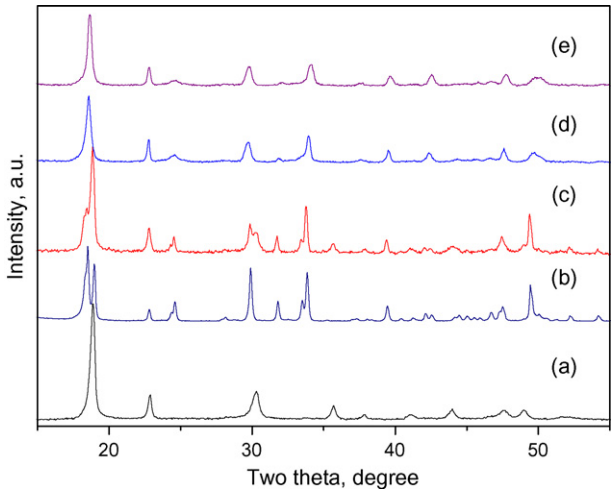

Fig. 1. X-ray diffraction patterns of (a) $NiC_2O_4{\cdot}2H_2O$; (b) α-$MnC_2O_4{\cdot}2H2O$; (c) mechanical mixture; (d) $Ni_{0.11}Mn_{0.89}C_2O_4{\cdot}2H_2O$ (phase II); (e) $Ni_{0.34}Mn_{0.66}C_2O_4{\cdot}2H_2O$ (phase I).

stable α-form, if they have been synthesized by "a soft chemical method". The studies [7,8] are focused on the ternary system $Ni_xCu_yMn_{(1-x-y)}C_2O_4{\cdot}2H_2O$ and on the basis of the progressing disappearance of some diffraction peaks the authors conclude that there is a transition from the α-form into the β-form, which is associated with the increased content of Ni at a constant amount of Cu. For the system $Ni_xCu_{0.1}Mn_{(0.9-x)}C_2O_4{\cdot}2H_2O$ they have found that at $x \leq 0.09$ the system is crystallizing in the monoclinic α-form, while at $x \geq 0.23$ the system crystallizes already in the orthorhombic β-form [7]. The X-ray diffraction patterns of the solid solutions, obtained by us (Fig. 1d and e), correspond visually to those, which are given in [7] as typical XRD patterns for the β-form. However the precise processing in the evaluating of the crystal lattice parameters shows that the solid solutions, studied by us $Ni_xMn_{1-x}C_2O_4{\cdot}2H_2O$ with $x = 0.10$ and 0.34, crystallize in the monoclinic α-form. Table 1 lists the parameters of the crystal lattice, determined by using the Powder Cell computer program [26].

3.2. Electron microscope investigation

Fig. 2 represents electron micrographs of the synthesized phases, corresponding to the X-ray patterns. It is clearly seen that two quite different types of crystals are present in the mechanical mixture—the small ones belong to $NiC_2O_4{\cdot}2H_2O$, while the big ones represent α-$MnC_2O_4{\cdot}2H_2O$. The photos of phases I and II show that the habitation and the size of the crystals differ from each other and from those of the individual oxalates. The micrographs also attend to the fact that the morphology and size are influenced by (i) the excess of oxalate ions, because the crystal habitation observed by us differs from that, obtained with stoichiometric amount of $C_2O_4^{2-}$ in the system [4,6,8]; (ii) the ratio Ni/Mn. The differences are visible even by means of an optical microscope at the 15th minute since the beginning of the synthesis. The crystals of the phase with

Table 1
Crystal lattice parameters of the samples, shown in Fig. 1.

Samples	Lattice constants a–c (Å) and β (°)			
	$a \pm 0.002$	$b \pm 0.002$	$c \pm 0.002$	$\beta \pm 0.15$
Ref. JCPDS 25-0544	12.016	5.632	9.961	128.4
$MnC_2O_4{\cdot}2H_2O$ (1:1)	11.99	5.644	9.975	128.36
$Ni_{0.11}Mn_{0.89}C_2O_4{\cdot}2H_2O$	12.034	5.612	9.889	127.75
$Ni_{0.34}Mn_{0.66}C_2O_4{\cdot}2H_2O$	12.02	5.592	9.857	127.57

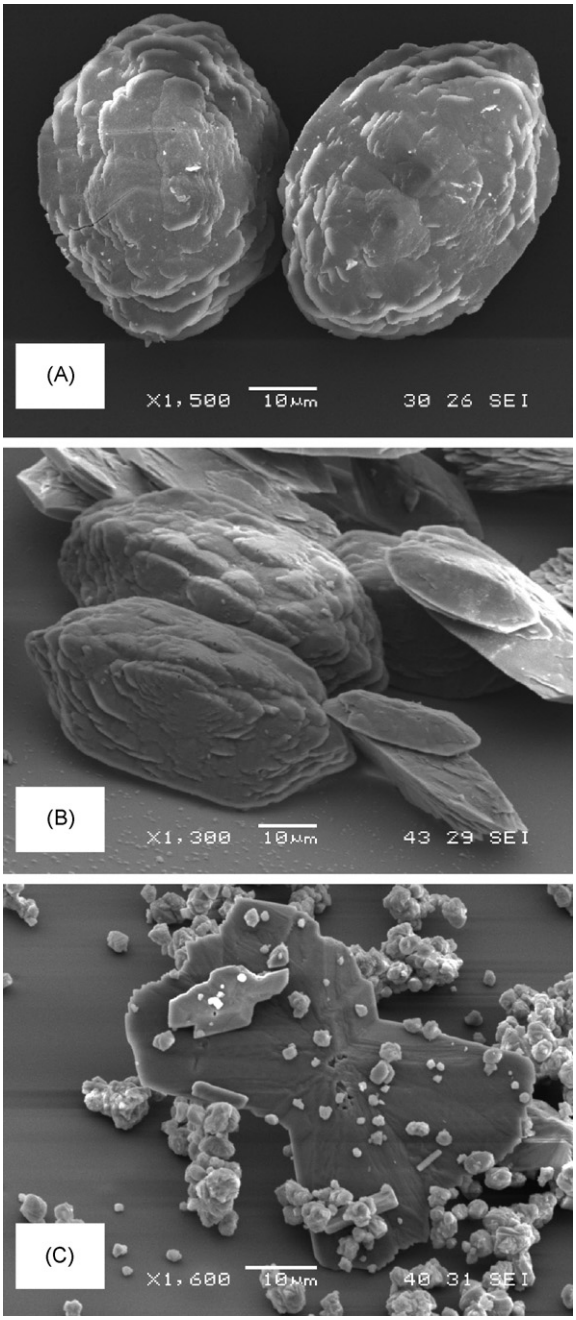

Fig. 2. Electron micrographs of (A) $Ni_{0.11}Mn_{0.89}C_2O_4{\cdot}2H_2O$ (phase II); (B) $Ni_{0.34}Mn_{0.66}C_2O_4{\cdot}2H_2O$ (phase I); (C) mechanical mixture.

higher content of Ni ($Ni_{0.34}Mn_{0.66}C_2O_4{\cdot}2H_2O$) are smaller in size, but the facets are better in form, the shape is more regular with a factor of anisometry 1.73. The phase with lower content of Ni ($Ni_{0.11}Mn_{0.89}C_2O_4{\cdot}2H_2O$) is not so well shaped and the anisometric factor is 1.33. This result shows that the ratio Ni/Mn influences not only the parameters of the crystal lattice, but also the morphology.

3.3. Thermal analysis

As it was stated above, the decomposition mechanism of $NiC_2O_4{\cdot}2H_2O$ and $MnC_2O_4{\cdot}2H_2O$ is not one and the same [21,22,27–35]. In the first case an elemental nickel is produced and in oxidative atmosphere it forms NiO. In the second case the decomposition leads to oxide forming. The temperatures of dehydration

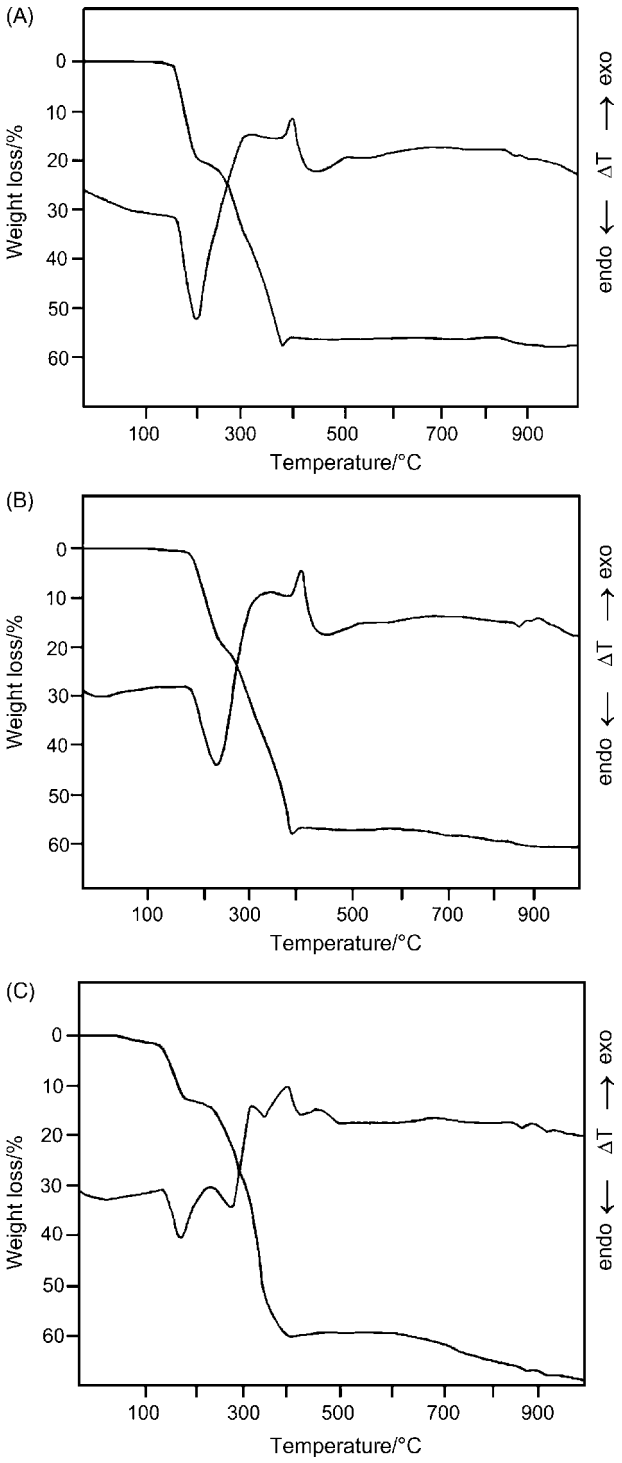

Fig. 3. DTA and TGA profiles for: (A) $Ni_{0.11}Mn_{0.89}C_2O_4{\cdot}2H_2O$ (phase II); (B) $Ni_{0.34}Mn_{0.66}C_2O_4{\cdot}2H_2O$ (phase I); (C) mechanical mixture.

and decomposition depend most of all on the strength of bonding M–O(H_2O) and that of M–O(C_2O_4) [21,22,35], on the kind of atmosphere, in which the process is occurring, on the inclination of the M^{2+} ion to be oxidized [21,22,30,31], as well as on the specific conditions (the charged mass of the sample, the rate of heating, the form of the vessel, etc.).

Fig. 3 represents the results of the thermal analysis (in air) for the mechanical mixture, for phase I – $Ni_{0.34}Mn_{0.66}C_2O_4{\cdot}2H_2O$ and for phase II – $Ni_{0.11}Mn_{0.89}C_2O_4{\cdot}2H_2O$.

It is known that $NiC_2O_4{\cdot}2H_2O$ tends to crystallize with sorption bonded water molecules. In accordance with this fact it is observed that such type of bonded water is liberated (~2%) at temperatures higher than 60 °C in case of mechanical mixture (Fig. 3C). The next experimental loss of weight (~20%) for this sample is associated with step-by-step dehydration of α-$MnC_2O_4{\cdot}2H_2O$ (175 °C) and that of $NiC_2O_4{\cdot}2H_2O$ (275 °C). The last one does not proceed completely as it was established in Refs. [33,34]. That is why the end of $NiC_2O_4{\cdot}2H_2O$ dehydration overlaps with the beginning of the mechanical mixture decomposition. This decomposition gives rise to a set of peaks at 340 °C (exo-peak) and 360 °C (endo-peak), 410 °C (exo-peak) and 460 °C (endo-peak), which correspond to the decomposition of the two oxalates. No interaction is observed in the course of this process. A minimum is visible in the TG-curve, which is not connected with the decomposition of the α-$MnC_2O_4{\cdot}2H_2O$ [23], used for preparing the mechanical mixture. The presence of such a minimum is characteristic of oxalates of Ni, Co, Cu [21,24] and it is associated with the formation of elemental Ni, which is immediately oxidized in air atmosphere. In the specific case the minimum is not so clearly expressed because of the superimposition of the separate oxalates decompositions. The obtained oxide products interact at temperatures above 800 °C forming a spinel phase $NiMn_2O_4$. The theoretically calculated decrease is 67.5%, while the experimentally observed one is 68.5%.

The thermal analysis of the phases II and I (Fig. 3A and B) indicates that they display behavior characteristic of a separate chemical compound, i.e. they are real solid solutions. The dehydration occurs in a single step and the process of decomposition results in two exo-peaks, which is in correspondence with the results, obtained in [5]. For the compound $Ni_{0.11}Mn_{0.89}C_2O_4{\cdot}2H_2O$ (phase II) the peaks, obtained in the present study, are located at 200 °C, 320 °C, 400 °C, while for $Ni_{0.34}Mn_{0.66}C_2O_4{\cdot}2H_2O$ (phase I)—at 225 °C, 335 °C, 415 °C. It is seen that a little increase in the amount of Ni leads to an increase in the temperature of dehydration (T_{deh}) and in the temperature of decomposition (T_{decomp}). The reason for the increase in T_{deh} is the increase in the bond energy M–O(H_2O) in axial position in the sequence from Mn to Ni [35,37]. In this direction the bond in equatorial position M–O(C_2O_4) is growing weaker, which should lead to lowering of the decomposition temperature upon increasing the quantity of Ni. If, however, the decomposition occurs in an oxidative atmosphere it is known that T_{decomp} of the 3d-element oxalates does not decrease, but increases in the sequence from Mn to Ni, which is connected with decreasing in the M^{2+} oxidation ability [27,30,31]. For this reason during the decomposition in air phase I (with lower content of Mn^{2+}) is dehydrated and decomposed at higher temperatures.

At the end of the decomposition processes of the solid solutions the TG-curves resemble a lot that of the mechanical mixture. Therefore it can be supposed the liberated CO reduces not only Mn^{n+} [23], but also the Ni^{n+}. (This could explain also the dependence of the cation deficiency in the spinels on the nickel content, reported in the literature.) The consecutive oxidation of the obtained products leads to a stronger second exo-peak compared to the same observed with the pure $MnC_2O_4{\cdot}2H_2O$ sample [23].

3.4. Mass-spectral analysis of the evolved gases (EGA)

The results from the mass-spectral analyses of the gaseous products, obtained in the course of decomposition of $Ni_xMn_{1-x}C_2O_4{\cdot}2H_2O$ under reduced pressure in vacuum ($p \leq 1 \times 10^{-3}$ Torr) are illustrated in Fig. 4. The comparison of the decomposition of the individual transition metal oxalates in air and in vacuum has been done in Refs. [27,31]. It has been shown that for $MnC_2O_4{\cdot}2H_2O$ T_{deh} is almost one and the same in both media, but T_{decomp} is strongly increased in vacuum. In

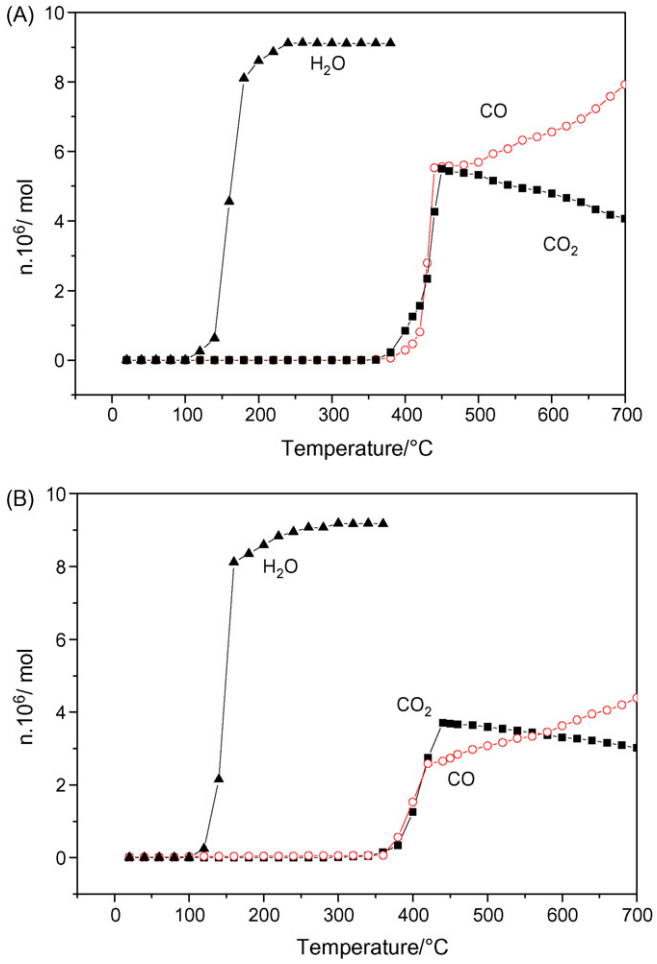

Fig. 4. Mass-spectral analyses of (A) $Ni_{0.11}Mn_{0.89}C_2O_4{\cdot}2H_2O$ (phase II); (B) $Ni_{0.34}Mn_{0.66}C_2O_4{\cdot}2H_2O$ (phase I).

the case of $NiC_2O_4{\cdot}2H_2O$, however, T_{deh} is strongly decreased in vacuum, while T_{decomp} is almost unchanged. In accordance with this observation are the temperature intervals represented in Table 2. The comparison with the DTA data indicates that the dehydration process of the both solid solutions in vacuum starts at a lower temperature in regard to the starting temperature in air. The comparison between T_{decomp} of the phase I and phase II confirms that when the oxidation of M^{2+} does not exert any effect, the energy of the bond M–O(C_2O_4) is of importance for the temperature of decomposition. As was mentioned above the strength of this bond decreases in the sequence from Mn to Ni [22,35–37]. That is why in vacuum the phase I, which has a lower content of Mn^{2+} is decomposed at a lower temperature than the phase II—$Ni_{0.11}Mn_{0.89}C_2O_4{\cdot}2H_2O$.

According to the literature data in vacuum the individual oxalates decompose as follows: nickel oxalate produces Ni and CO_2, while the manganese oxalate—MnO + CO + CO_2. As it is seen in Fig. 4 after the initial dehydration of $Ni_xMn_{1-x}C_2O_4{\cdot}2H_2O$, the samples

Table 2
Temperature intervals of dehydration (ΔT_{deh}) and decomposition (ΔT_{decomp}), the ratio nCO/nCO_2 at the end of the process of decomposition of $Ni_{0.11}Mn_{0.89}C_2O_4{\cdot}2H_2O$ and $Ni_{0.34}Mn_{0.66}C_2O_4{\cdot}2H_2O$ in vacuum.

Samples	ΔT_{deh}	ΔT_{decomp}	nCO/nCO_2 (T^f_{decomp})
$Ni_{0.11}Mn_{0.89}C_2O_4{\cdot}2H_2O$	110–200	360–460	1:1
$Ni_{0.34}Mn_{0.66}C_2O_4{\cdot}2H_2O$	110–160	340–440	2.63/3.7

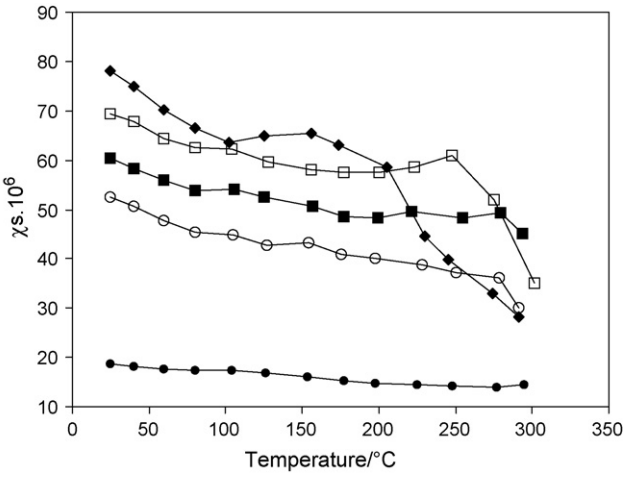

Fig. 5. Temperature dependence of the specific magnetic susceptibility of $NiC_2O_4{\cdot}2,2H_2O$ (●), α-$MnC_2O_4{\cdot}2H_2O$ (♦), mechanical mixture (○), $Ni_{0.11}Mn_{0.89}C_2O_4{\cdot}2H_2O$ (□) and $Ni_{0.34}Mn_{0.66}C_2O_4{\cdot}2H_2O$ (■).

are further decomposed in a single step. (This fact confirms that the second peaks in the DTA curves are due to oxidation processes occurring in air.) In the case of sample $Ni_{0.11}Mn_{0.89}C_2O_4$, containing a smaller quantity of Ni, at the end of the decomposition process almost equivalent amounts of CO and CO_2 are obtained. This result is in accordance with the result obtained for the thermal decomposition of MnC_2O_4 [30–32,35]. Due to the presence of nickel the excess of CO_2 over CO is expected but this excess is too small to be detected by mass-spectral analysis of this sample. In the case of the sample $Ni_{0.34}Mn_{0.66}C_2O_4$, however, the obtained CO_2 is more than the CO, and it is logically due to the reduction of Ni^{n+}. This confirms the conclusion, based on the DTA analysis, that the minimum in the TG-curve is a result of reduction to elemental Ni, which later undergoes oxidation.

The increase in the amount of CO after the end of the decomposition process is connected with the strongly reducing conditions, created in the reaction vessel. Part of the liberated water is reduced to H_2, whose presence is proven by the analysis of the gas mixture obtained. A part of the formed molecular hydrogen reacts further with the liberated CO_2 and reduces it.

3.5. Magnetic measurements in situ

Fig. 5 represents the temperature dependences of the specific magnetic susceptibility (χ_s) of the studied samples in the temperature interval 25–300 °C *in situ*. The decrease in χ_s upon increasing the temperature shows that the samples are paramagnetic.

The magnetic susceptibility allows calculating the values of the effective magnetic moments (μ_{eff}) and the values of the constant of Weiss (θ). While the magnetic moment enables the determination of the oxidation state of the metal, the Weiss constant depends on the environment of the given ion and it is used to monitor changes in the character of interaction between the metal ions [38–41]. The theoretical values of μ^0_{eff} in case of octahedral intermediate field for the various oxidation states of manganese are 5.92 BM for Mn(II), 4.70 BM for Mn(III) and 3.44 BM for Mn(IV) and they do not depend on the temperature [41]. According to the contemporary theoretical concepts, μ_{eff} of Ni^{2+} in octahedral crystal field does not depend on the temperature and it has a value of 3.28 BM at $\Delta = 8000\,cm^{-1}$, while μ_{eff} of Ni^{3+} is 5.13 BM and it depends on the temperature. In tetrahedral crystal field μ_{eff} for Ni^{2+} depends on the temperature and at 300 K it has a value of 3.97 BM, while μ_{eff} for Ni^{3+} does not depend on the temperature and it has a value of 4.33 BM [38–41].

Table 3
Experimental (μ_{eff}) and theoretical (μ^0_{eff}) effective magnetic moments (for Oh field) of the studied samples within the interval 25–80 °C for $MnC_2O_4{\cdot}2H_2O$, $NiC_2O_4{\cdot}2{,}2H_2O$, their mechanical mixture and the phases $Ni_{0.34}Mn_{0.66}C_2O_4{\cdot}2H_2O$ and $Ni_{0.11}Mn_{0.89}C_2O_4{\cdot}2H_2O$.

No.	Samples	μ_{eff} (BM)	μ^0_{eff} (BM)	θ (K)
1	α-$MnC_2O_4{\cdot}2H_2O$	5.92	5.92	−13
2	$Ni_{0.11}Mn_{0.89}C_2O_4{\cdot}2H_2O$	5.46	5.70	−26
3	$Ni_{0.34}Mn_{0.66}C_2O_4{\cdot}2H_2O$	5.12	5.17	−6
4	Mechanical mixture	4.85	4.8	6
5	$NiC_2O_4{\cdot}2{,}2H_2O$	2.95	3.28	−70

Table 4
The weight loss during dehydration (Δm_{deh},%) and the temperatures at which the dehydration finishes (T^f_{deh}), the decomposition starts (T^f_{decomp}) and a considerable change in the value of μ_{eff} occurs ($T^{in}_{(\Delta\mu)}$).

No.	Samples	Δm_{deh} (%)	T^f_{deh}	T^{in}_{decomp}	$T^{in}_{(\Delta\mu)}$
1	α-$MnC_2O_4{\cdot}2H_2O$	−20	160	215.35	21.35
2	$Ni_{0.11}Mn_{0.89}C_2O_4{\cdot}2H_2O$	−20	191.63	191.63	>247.5
3	$Ni_{0.34}Mn_{0.66}C_2O_4{\cdot}2H_2O$	−20	206.79	206.79	>279.5
4	Mechanical mixture	I: −12 II:	162.71 >300	Superposition of 2 processes	>278.5
5	$NiC_2O_4{\cdot}2{,}2H_2O$	−21.20	>300		>300

Table 3 lists the values of the magnetic moments (μ_{eff}) and the values of Weiss constant (θ), calculated on the basis of the Law of Curie-Weiss Eq. (1) for the temperature interval 25–80 °C. For comparison the table represents also the theoretically calculated values for these systems (μ^0_{eff}). The comparison indicates that the manganese and nickel are in oxidation state +2. The negative values of θ show that the magnetic interaction belongs to the antiferromagnetic type. The exchange interaction between the ions in the crystal lattice is weak, as the values of θ are not high. For the mechanical mixture θ is positive, but this is determined by the fact that the system has two phases. Due to the close values of θ of the two pure phases, included in the mechanical mixture, the Law of Curie-Weiss is followed as well. The results from the magnetic measurements confirm that the samples, obtained by co-crystallization, are real solid solutions.

Fig. 6A represents the change in the effective magnetic moments within the temperature interval 25–300 °C. The calculations have been made using Eq. (1) at a constant value of θ and taking into account the change in the weight of the sample (Fig. 6B) in the course of the magnetic measurements.

As the magnetic moment of a given metal ion depends on its oxidation state, its coordination and the force of the crystal field, then the change in the magnetic moment reflects the changes, which occur in the studied sample upon increasing the temperature. In order to analyze the change in the magnetic moment the sample dehydration should be distinguished from the process of its decomposition. It is evaluated on the basis of the weight loss (Table 4). The table lists the temperature, at which the dehydration is completed (T^f_{deh}) as well as the temperature, at which the process of decomposition (T^{in}_{decomp}) starts. The temperature, at which a considerable change in the value of μ_{eff} occurs ($T^{in}_{(\Delta\mu)}$), is also represented.

It is seen from Fig. 6A that in the initial stage of the process of dehydration of the samples (up to $T \sim 80$ °C) the μ_{eff} values are preserved relatively constant and therefore no changes in the oxidation state of M^{2+} in the samples are occurring. Above this temperature a weak increase of the μ_{eff} values is observed for all the samples. As the process of dehydration, however, is not complete yet this increase of the μ_{eff} values is associated not with the change in the oxidation state of the manganese or nickel, but with the change in Weiss constant.

After the dehydration a process of decomposition starts. The temperatures obtained in the course of magnetic measurements (in air) confirm the conclusions, drawn as a result of the analysis of the DTA-curves: (i) presence of Ni leads to a decrease in T_{decomp} in regard to that of the pure manganese oxalate and (ii) upon increasing the nickel in the solid solution T_{decomp} is growing up.

In the course of decomposition changes in the magnetic moments are expected due to changes in the coordination and in the oxidation state of manganese and nickel. The oxidation of Mn^{2+} would lead to a decrease in μ_{eff}, while the oxidation of Ni^{2+}—to an increase in μ_{eff}. In spite of the low content of Ni in the studied samples the juxtaposition of the results with those for α-$MnC_2O_4{\cdot}2H_2O$ [23] indicates its effect. In case of α-$MnC_2O_4{\cdot}2H_2O$ in parallel with the decrease of the mass as a result of the decomposition process there starts an irreversible decrease in μ_{eff} due to the oxidation of Mn^{2+} to Mn^{3+}, Mn^{4+} [23]. There is not such a parallel in the studied systems. It is seen in Fig. 6A that in both cases of solid solutions after T_{decomp} there is a weak decrease in μ_{eff} due to the oxidation of Mn^{2+}, which has a stronger oxidation ability than Ni^{2+} [30]. However afterwards a weak increase in μ_{eff} is observed, which is most probably due to the oxidation of Ni^{2+} to Ni^{3+}. Due to the low content of nickel in the samples this effect is comparatively weak. The increase continues further to a temperature, corresponding to almost one half degree of decomposition (mass loss ~15%). It is interesting that if we compare this loss of mass to the data from DTA it will become clear that the first exothermal peak in the respective curves is at

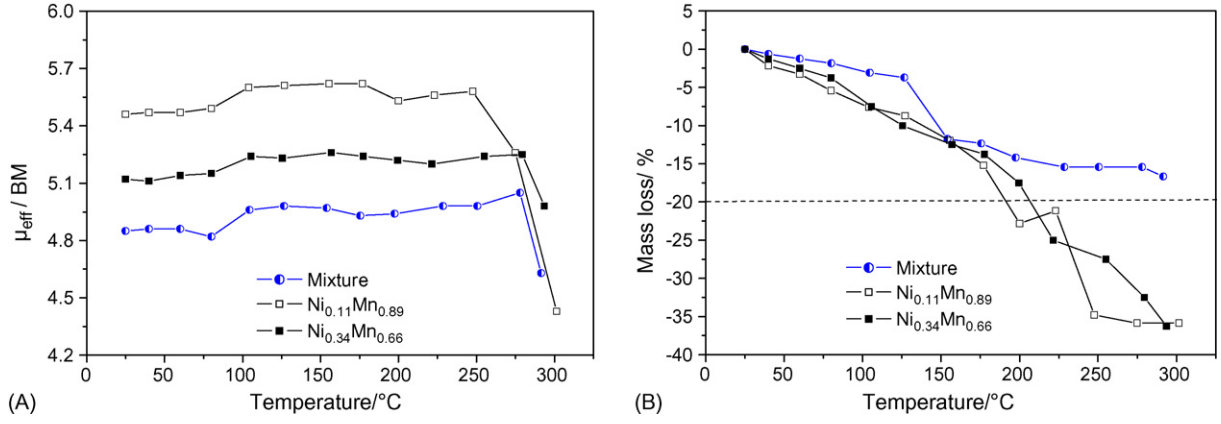

Fig. 6. Temperature dependence of the magnetic moments (A) and the weight during *in situ* magnetic measurements (B) of $Ni_{0.11}Mn_{0.89}C_2O_4{\cdot}2H_2O$ (phase II), $Ni_{0.34}Mn_{0.66}C_2O_4{\cdot}2H_2O$ (phase I) and mechanical mixture.

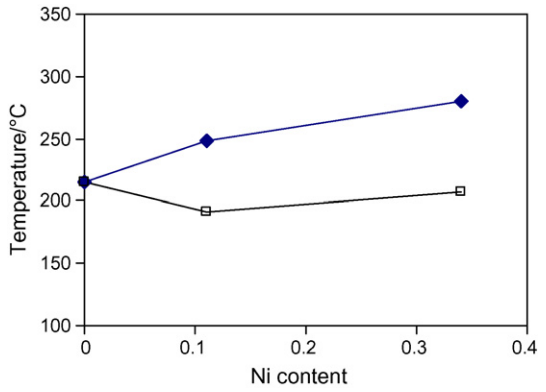

Fig. 7. Dependence of T^{in}_{decomp}: (□) (the initial temperature of decomposition) and $T^{in}_{(\Delta\mu)}$: (♦) (the temperature, at which the considerably change in the value of μ_{eff} occurs) on the nickel content.

~15% reduction of the weight. Therefore in the temperature interval ($T^{in}_{decomp} - T^{in}_{(\Delta\mu)}$), which corresponds to a half degree of decomposition the process of oxidation of Ni^{2+} determines the change of μ_{eff}. It is only afterwards that the process of oxidation of Mn (or reduction of Ni) becomes dominating. Therefore, the presence of nickel in the partially decomposed samples leads to stabilization of Mn^{2+}. Such a stabilizing effect against oxidation has also been observed in the case of substitution of manganese with zinc in the spinel structure of $Zn_xMn_{3-x}O_4$ [42]. It is associated with the fact that the highly energetic bond Zn–O decreases the cation migration in the lattice.

The influence of nickel is best illustrated in Fig. 7, which represents T^{in}_{decomp} and $T^{in}_{(\Delta\mu)}$ as a function of its content. In summary, the conclusions are as follows: (i) the presence of Ni in $Ni_xMn_{1-x}C_2O_4{\cdot}2H_2O$ leads to decreasing in the decomposition temperature in regard to that of the manganese oxalate; (ii) upon increasing the Ni content the temperature of decomposition in air is growing up; (iii) the presence of Ni stabilizes the manganese with respect to oxidation, in spite of the occurring process of decomposition.

From the data obtained by the magnetic measurements, DTA/TG and mass-spectral analysis one can suppose the following mechanism of the change of the oxidation state of the ions depending on the temperature and the degrees of dehydration and decomposition:

Up to 100 °C	Dehydration	Decomposition	
Ni^{2+}	$\longrightarrow$ Ni^{2+}	$\longrightarrow$ Ni^{2+}, Ni^{3+}	$\longrightarrow$ Ni^{2+}
Mn^{2+}	$\longrightarrow$ Mn^{2+}	$\longrightarrow$ Mn^{2+}, Mn^{4+}	$\longrightarrow$ Mn^{2+}, Mn^{3+}, Mn^{4+}

This mechanism confirms the reported possibility of forming ilmenite phase $NiMnO_3$ at low temperatures and the formation of spinel phase $NiMn_2O_4$ at high temperatures. The stoichiometry of the spinel phase is determined by the ratio Ni/Mn in the initial oxalate, accounting for the presence of nickel ions Ni^{3+} and ions of manganese Mn^{2+}, Mn^{4+}.

4. Conclusion

The results from the thermal magnetic measurements show and confirm that the synthesized samples with composition $Ni_{0.34}Mn_{0.66}C_2O_4{\cdot}2H_2O$ and $Ni_{0.11}Mn_{0.89}C_2O_4{\cdot}2H_2O$ are real solid solutions. The XRD and SEM analyses show that (i) they are iso-structural to α-$MnC_2O_4{\cdot}2H_2O$; (ii) the excess of oxalate ions influences the morphology of the crystal phase; (iii) the ratio Ni/Mn influences the rate of growth of the separate facets.

The thermal analysis, the EGA-MS investigation and the magnetic measurements confirmed that the changes in the temperatures of dehydration and decomposition depend on the medium, in which the process is occurring, as well as on the quantity of Ni. The evolved gas analysis indicates a regular decrease in the amount of liberated CO upon increasing the Ni content in the sample. These results followed the theoretical dependences, established for the oxalates of 3d-elements.

In the case of decomposition of the oxalates it can be expected that the liberated CO will have a reducing effect. In case of a presence of nickel in the system this reducing effect could lead to the formation of elemental nickel. Although there is indirect evidence about this statement (the course of the TG-curves and the EGA mass-spectral results) the magnetic measurements prove that in an oxidative medium, even if the reduction occurs, the re-oxidation of the nickel is a faster process. The possible reason for it is the high catalytic activity of the mixed oxide phase in regard to the oxidation of CO. An interesting result from the magnetic measurements is that while in the case of the manganese oxalate the change in the oxidation state is occurring at the moment of the sample decomposition, in the case of the studied solid solutions this change is connected with the degree of the sample decomposition. It shows that the nickel stabilizes the manganese with respect to oxidation.

Acknowledgement

The authors are thankful to Prof. K. Petrov for interpretation of XRD data.

References

[1] X.-X. Tang, A. Manthiram, J.B. Goodenough, J. Less-Common Met. 156 (1989) 357–368.
[2] A. Feltz, J. Töpfer, Z. Anorg. Allg. Chem. 576 (1989) 71–80.
[3] J. Töpfer, J. Jung, Thermochim. Acta 202 (1992) 281–289.
[4] S. Guillemet-Fritsch, M. Aoun-Habbache, J. Sarrias, A. Rousset, N. Jongen, M. Donnet, P. Bowen, J. Lemaitre, Solid State Ionics 171 (2004) 135–140.
[5] O.I. Gyrdasova, G.V. Bazuev, V.N. Krasil'nikov, V.A. Sharov, Russ. J. Inorg. Chem. 48 (2003) 1310–1315.
[6] C. Chanel, S. Fritsch, C. Drouet, A. Rousset, M.L. Martínez Sarrión, L. Mestres, M. Morales, Mater. Res. Bull. 35 (2000) 431–439.
[7] C. Drouet, P. Alphonse, A. Rousset, Solid State Ionics 123 (1999) 25–37.
[8] C. Drouet, P. Alphonse, J. Mater. Chem. 12 (2002) 3058–3063.
[9] C. Laberty, M. Verelst, P. Lecante, P. Alphonse, A. Mosset, A. Rousset, J. Solid State Chem. 129 (1997) 271–276.
[10] C. Laberty, J. Pielazok, P. Alphonse, A. Rousset, Solid State Ionics 110 (1998) 293–302.
[11] C. Drouet, C. Laberty, J.L.G. Kierro, P. Alphonse, A. Rousset, Int. J. Inorg. Mater. 2 (2000) 419–426.
[12] S. Fritsch, J. Sarrias, M. Brieu, J.J. Couderc, J.L. Baudour, E. Snoeck, A. Rousset, Solid State Ionics 109 (1998) 229–237.
[13] R. Schmidt, A. Stiegelschmitt, A. Roosen, A.W. Brinkman, J. Eur. Ceram. Soc. 23 (2003) 1549–1558.
[14] R. Schmidt, A. Basu, A.W. Brinkman, J. Eur. Ceram. Soc. 24 (2004) 1233–1236.
[15] R. Legros, R. Metz, A. Rousset, J. Mater. Sci. 25 (1990) 4410–4414.
[16] A. Rousset, R. Legros, A. Lagrange, J. Eur. Ceram. Soc. 13 (1994) 185–195.
[17] C. Laberty, C. Marquez-Alvarez, C. Drouet, P. Alphonse, C. Mirodatos, J. Catal. 198 (2001) 266–276.
[18] C. Drouet, P. Alphonse, A. Rousset, Appl. Catal. B: Environ. 33 (1) (2001) 35–43.
[19] R. Deyrieux, C. Berro, A. Peneloux, Bull. Soc. Fr. Mineral. Cristallogr. 1 (1973) 25–34.
[20] B. Donkova, J. Pentsheva, M. Djarova, Cryst. Res. Technol. 39 (3) (2004) 207–213.
[21] D. Dollimore, Thermochim. Acta 117 (1987) 331–363.
[22] M.A. Mohamed, A.K. Galwey, S.A. Halawy, Thermochim. Acta 429 (2005) 57–72.
[23] B. Donkova, D. Mehandjiev, Thermochim. Acta 421 (1–2) (2004) 141–149.
[24] B. Donkova, D. Mehandjiev, J. Mater. Sci. 40 (2005) 3881–3886.
[25] D. Mehandjiev, E. Nikolova-Zhecheva, Thermochim. Acta 77 (1980) 145–154.

[26] V. Kraus, J. Nolze, Powder Cell, version 2.4, 2000.
[27] G. Bakcsy, A.J. Hegedüs, Thermochim. Acta 10 (1974) 399–408.
[28] W.R. Pease, R.L. Segall, R.St.C. Smart, P.S. Turner, J. Chem. Soc., Faraday Trans. I 82 (1986) 747–758.
[29] D. Dollimore, Themochim. Acta 177 (1991) 59–75.
[30] E.D. Maclein, J. Inorg. Nucl. Chem. 30 (1968) 2689–2695.
[31] M.E. Brown, D. Dollimore, A.K. Galwey, J. Chem. Soc., Faraday Trans. 1 (70) (1974) 1316–1324.
[32] B. Małeska, E. Drożdż-Sieśla, P.K. Olszewski, J. Therm. Anal. Calorim. 74 (2003) 485–490.
[33] B. Małeska, A. Małeski, E. Drożdż-Sieśla, L. Torter, P. Llewellyn, F. Rouquerol, Thermochim. Acta 466 (2007) 57–62.
[34] C.S. Carney, C.J. Gump, A.W. Weimer, Mater. Sci. Eng. A 431 (2006) 1–12.
[35] K. Nagase, K. Sato, N. Tanaka, Bull. Chem. Soc. Jpn. 48 (2) (1975) 439–443.
[36] M.A. Mohamed, A.K. Galwey, Thermochim. Acta 217 (1993) 263–276.
[37] V.A. Sharov, T.M. Zhdanovskih, E.A. Nikonenko, Zh. Neorg. Khim. 24 (1979) 1489–1493 (Russ.).
[38] F.E. Mabs, D.J. Machin, Magnetism and Transition Metal Complexes, first ed., Chapman & Hall, London, 1973, p. 153.
[39] A. Earnshaw, Introduction to Magnetochemistry, first ed., Academic Press, London, New York, 1968.
[40] R. Boca, Theoretical Foundations of Molecular Magnetism, first ed., Elsevier, Amsterdam, Lousanne, New Yok, Oxford, Shannon, Singapore, Tokyo, 1999, p. 504.
[41] D. Mehandjiev, S. Angelov, Magnetochemistry of Solid State, first ed., Nauka i Izkustvo, Sofia, 1979, p. 116.
[42] S. Guillemet-Fritsch, C. Chanel, J. Sarrias, S. Bayonne, A. Rousset, X. Alcobe, M.L. Martinez Sarrión, Solid State Ionics 128 (2000) 233–242.